NASA Technical Memorandum 106842
AIAA–94–2849

NASA 30 cm Ion Thruster Development Status

Michael J. Patterson, Thomas W. Haag, and Vincent K. Rawlin
National Aeronautics and Space Administration
Lewis Research Center
Cleveland, Ohio

and

Michael T. Kussmaul
NYMA, Inc.
Engineering Services Division
Brook Park, Ohio

Prepared for the
30th Joint Propulsion Conference
cosponsored by AIAA, ASME, SAE, and ASEE
Indianapolis, Indiana, June 27–29, 1994

National Aeronautics and
Space Administration

NASA 30 cm Ion Thruster Development Status

Michael J. Patterson*, Thomas W. Haag*, and Vincent K. Rawlin*
National Aeronautics and Space Administration
Lewis Research Center
Cleveland, Ohio

Michael T. Kussmaul†
NYMA, Inc.
Engineering Services Division
Brook Park, Ohio

A 30 cm diameter xenon ion thruster is under development at NASA to provide an ion propulsion option for missions of national interest and it is an element of the NASA Solar Electric Propulsion Technology Applications Readiness (NSTAR) program established to validate ion propulsion for space flight applications. The thruster has been developed to an engineering model level and it incorporates innovations in design, materials, and fabrication techniques compared to those employed in conventional ion thrusters. The performance of both functional and engineering model thrusters has been assessed including thrust stand measurements, over an input power range of 0.5-2.3 kW. Attributes of the engineering model thruster include an overall mass of 6.4 kg, and an efficiency of 65% and thrust of 93 mN at 2.3 kW input power. This paper discusses the design, performance, and lifetime expectations of the functional and engineering model thrusters under development at NASA.

Nomenclature

F	= thrust, N
F_t	= thrust-loss correction factor due to beam divergence
I^+	= singly-charged ion beam current, A
I^{++}	= doubly-charged ion beam current, A
J_b	= ion beam current, A
m	= ion mass, kg
q	= ion charge, C
R	= net-to-total acceleration voltage ratio
V_b	= beam voltage, V
V_g	= floating potential of neutralizer-common with respect to facility ground, V
V_s	= screen grid voltage, V
α	= thrust-loss correction factor for doubly-charged ions
γ	= total thrust-loss correction factor

Introduction

Several flight experiments and demonstrations of ion propulsion are being conducted by the Europeans and Japanese during this decade.[1-3] In the United States, NASA has a program to develop ion thruster system technologies to satisfy auxiliary and primary propulsion requirements for missions of national interest.

To date, a series of test programs has been conducted at NASA with laboratory version 30 cm ion thrusters and components to establish a database for development of an engineering model thruster.[4-14] Goals of the engineering model thruster development effort include a thruster mass of ≤ 7 kg and an operating power envelope of 0.5 to 5.0 kW.

Most recently, the thruster hardware was developed to a functional model level of maturity.[15] The thruster incorporated major innovations in structural design, materials, and fabrication techniques compared to those employed in conventional ion thrusters, including an all-aluminum, partial-conic discharge chamber design. Performance data for the thruster were obtained over a 0.7-4.9 kW power envelope and the results verified the design approach.

Subsequent to this effort, additional performance assessments of the functional model thruster (FMT) were conducted to evaluate its performance in detail over a 0.5-2.3 kW operating envelope at both high-efficiency and high thrust-to-power operating conditions. Additionally, direct-thrust measurements were obtained with the FMT over this input power level to verify thrust-loss estimates associated with beam divergence and multiply-charged ions.

Based on these results, an engineering model thruster (EMT) development program was initiated, the fabrication of the first of several thrusters was completed, and preliminary performance data were obtained over a 0.5-

---

*Aerospace Engineer, Member AIAA

†Aerospace Engineer

2.3 kW power envelope. This paper discusses recent performance data, including direct thrust measurements, obtained with the FMT. Additionally, the engineering model thruster design and preliminary performance data are also presented.

Thruster Design

The thruster hardware is shown in Figures 1 and 2. It has a configuration similar to that which may be used in a flight application and it is being used to validate the design. This engineering model thruster, or EMT, was preceded by a functional model thruster, or FMT, that was used to define manufacturing processes and to verify the physical and functional design. Table 1 compares attributes of the EMT and FMT. The overall mass of the EMT, including 3 m cable harness, is approximately 6.4 kg and is somewhat lighter than the FMT.

The EMT was developed with certain operational and performance goals and objectives. These include: an input power envelope of 0.5 kW to 2.3 kW, with a lifetime of 10,000 h; performance comparable to that demonstrated previously with the FMT and other 30 cm laboratory model thrusters[4-6,8,10,12,15]; design and interfaces that are compatible with the mission and system requirements for both auxiliary and primary propulsion applications; simplified power processing requirements; and reduced thruster size, mass (to approximately 7 kg), parts count, and fabrication costs.

The EMT of Figs. 1 and 2, and the earlier FMT, incorporates innovations in design, materials, and fabrication techniques compared to those employed in conventional thrusters. These include a conic discharge chamber which transitions into a short cylindrical region immediately upstream of the ion optics. This partial-conic design is inherently more rigid and occupies less volume than conventional cylindrical shape thrusters, while still exhibiting good discharge characteristics and promoting a uniform plasma distribution across the exit plane. Past development efforts have shown the large rear wall of cylindrical shape thrusters to be an inefficient stress-bearing structure and vulnerable to mechanical vibration.[16]

The use of non-ferromagnetic discharge chamber materials is a major departure from conventional ring-cusp thruster designs and previous thrusters. The engineering model thruster uses both 0.8 mm thick alloy 5052 aluminum and 0.5 mm thick AMS 4901 titanium for the discharge chamber, magnet retention rings, and other structural components. The use of aluminum and titanium, as opposed to steel, was motivated by a concern to reduce the thruster mass to an absolute minimum. This is because thruster mass reductions can create a 'ripple' effect that can significantly reduce the mass of a multi-thruster propulsion system.[17] An added advantage of aluminum is that the complex shape of the thruster can be readily fabricated using a spin forming technique, at relatively low cost. Both die stamping and spin forming were originally considered as each technique permits seamless formation of complex shapes from a single sheet of metal. Because of its lower initial tooling cost, metal spinning is often preferred for low volume production and was used for fabricating the thruster aluminum components described herein.

The discharge hollow cathode does not employ a keeper or starting electrode and discharge-coupling to the anode is used for ignition and steady-state operation. With the screen grid electrode electrically isolated, all cathode potential surfaces in the discharge chamber, except the hollow cathode assembly itself, are eliminated in the thruster design. This approach reduces the total number of components subjected to sputtering via discharge plasma ions to an absolute minimum.

The thruster uses a distributed 'reverse-injection' propellant manifold for the discharge chamber flow, where the propellant is introduced into the discharge chamber near the ion optics and directed backwards toward the cathode. The reverse-feed approach improves the propellant efficiency obtainable especially at throttled conditions, as compared to the conventional approach of introducing the propellant at the rear of the discharge chamber.

The EMT is designed to accommodate a simplified power processing approach. The thruster is normally operated using 4 commercial power supplies for steady-state operation, with 2 additional power supplies required for cathode conditioning, with a total of 7 power leads to the thruster. The breadboard power processor now under development will consist of a total of only 3 power supplies to operate the thruster. This further reduction in power processing requirements is implemented by combining functions performed by multiple power supplies into single custom modules, with the benefit of reduced parts count and mass.[18]

The magnetic circuit employed in the thruster is of ring-cusp design.[8] It uses high-field strength, rare-earth permanent magnets in rings of alternating polarity along the perimeter of the chamber, with the field lines terminating on anode potential surfaces. Three cusps are located in the discharge, one each in the regions of the discharge cathode, the discharge sidewall (at the conic-cylinder intersection), and the ion optics-end.

The discharge chamber and neutralizer cathode assemblies for the EMT consist of a hollow cathode assembly composed of a high temperature refractory alloy tube and an electron emitting insert impregnated with a low-work function compound. Both assemblies also use a sheathed heater design, derived from the mercury ion thruster, used for both activation and ignition of the cathodes.[16] The neutralizer cathode assembly incorporates an enclosed-keeper electrode design to improve gas efficiency, with critical design parameters established to maximize ion transparency and reduce beam-coupling potentials. Overall mass of the neutralizer assembly and its titanium

mounting bracket is approximately 250 grams.

The FMT and EMT ion optics systems are of a two-grid design which is derived from that developed for an engineering model mercury ion thruster.[16] The electrodes are fabricated from molybdenum and are dished outward. The electrodes are attached to thicker molybdenum stiffening rings, which are in turn attached to a titanium ring to form the ion optics assembly. The accelerator ring is electrically isolated from the titanium mounting ring with 12 equally spaced insulators. The titanium ring is in turn electrically isolated from the anode-potential discharge chamber via 6 equally space insulators. The mass of the FMT ion optics are approximately 2.43 kg, while those of the EMT are approximately 1.88 kg due to a modified titanium ring.

The FMT electrodes have nominal thicknesses of 0.38 mm for both the screen and accelerator grids, while on the EMT, the accelerator grid thickness was increased to 0.51 mm to permit reduced accelerator grid operating voltages and increase grid lifetime. Other features of the electrodes are identical for both thrusters. The apertures are of circular shape, with inner circle diameters of 1.91 mm and 1.14 for the screen and accelerator grids, respectively. The open-area-fractions are 0.67 and 0.24 for the screen and accelerator grid, respectively. The nominal cold grid gap is set at 0.66 mm. The screen grid hole pattern dimensions were reduced from those of the accelerator grid to reduce beam divergence losses. The electrode geometries for both thruster optics are listed in Table 2.

For purposes of performance characterizations and wear testing, the present EMT and the FMT use low-pressure high-voltage isolators. This approach results in a more complex thruster/propellant system interface than a high-pressure design but readily permits flow variations to accommodate throttling. Subsequent EM thrusters will incorporate a high-pressure high-voltage propellant isolator design.

The plasma screen of the EMT is fabricated from 0.25 mm thick 304 stainless steel. It is constructed of 3 separate pieces which are seam welded together to form a single unit. The stainless steel is chemically-etched to an open-area-fraction of about 50% with 0.51 mm diameter holes over about 80% of it's total surface, and it has a total mass of about 590 grams.

Support Equipment and Procedure

The thrust stand used in these tests was a calibrated displacement inverted pendulum design. A multiple flexure arrangement permitted up to 5 mm of horizontal movement along the sensing axis. Displacement from the neutral position was proportional to the thrust and was measured with a linear variable differential transformer. The resulting signal was then plotted as a function of time on a strip chart recorder. Force measurements were quantified by precisely comparing thrust induced deflection with those produced from a calibrated weight arrangement.

To accommodate the thrust stand measurements, propellant was transferred to the thruster through 3 flexible stainless steel tubes. These supplied xenon independently to the discharge cathode, main plenum, and the neutralizer cathode. Electrical power was transferred to the thruster through a commercially available flexure ribbon in which multiple flat conductors were laminated between two sheets of high voltage insulation. Seven conductive pathways were arranged to satisfy the electrical interface requirements of the thruster.

The procedure for taking thrust measurements began with establishing a zero point in which all propellant flow and power to the thruster was off. Calibration weights were then cycled to determine the thrust stand sensitivity. The thruster was then started and stabilized at the test point operating condition. Thrust levels were monitored from cold flow, through the nominal operating condition, and at thrust termination. Following approximately every fifth test point, the thrust stand zero was rechecked and the calibration weights were cycled again. The measured thrust values were then corrected for zero drift with the intermediate test points corrected by assuming a constant zero drift with time over the test period. The zero drift appeared to be independent of the thruster input power level, and at maximum, resulted in a reduction in the indicated thrust level by 2.2 mN which occurred over a test period of approximately 145 minutes. Based on repeatability and the magnitude of the zero drift, an uncertainty of $\pm$ 1.0 mN is estimated for the thrust measurement for each test point.

Laboratory power supplies were used for thruster performance testing.[4] The FMT and EMT use only 4 power supplies for steady-state operation, with 2 additional power supplies for the start-up of discharge and neutralizer cathodes. Discharge ignition was routinely obtained using open circuit voltage ($\leq$ 75 volts) of the discharge supply to initiate the cathode to anode discharge. Typical starting voltages for the neutralizer were $\leq$ 20 volts.

Tests were performed using high-purity xenon propellant. The propellant feed system used an all-electropolished stainless-steel tubing construction consisting of welds and metal-gasket seals. The three feed lines to the thruster (main, cathode, and neutralizer) incorporated individual commercial mass flow transducers to measure the propellant flow rate. Each transducer was calibrated using a primary standard.

Thruster performance testing was conducted in the Tank 5 vacuum chamber facility at NASA Lewis Research Center (LeRC). The chamber is 4.6 m in diameter by 19.2 m in length. The pumping characteristics of the facility include a maximum 340 kℓ/s xenon pumping speed (using twenty 0.9 m diameter oil diffusion pumps

and a 28 m^2 cryopanel), a no-load pressure of $\leq 6.7x10^{-5}$ Pa, and an operational pressure of $\leq 1.0x10^{-3}$ Pa.

The thrusters were operated under manual control for all performance testing. Data were recorded from calibrated digital metering. All thruster performance data were corrected for thrust losses associated with beam divergence and doubly-charged ions. Total efficiency and specific impulse calculations included losses associated with accelerator drain and neutralizer power, and neutralizer flow rate. All propellant efficiencies included a correction to the mass flow rate for propellant ingested from the facility. A detailed discussion of the thruster performance calculations can be found in reference 15. Those calculations specific to determination of thrust, including an uncertainty analysis, are discussed in the appendix.

Discharge chamber performance was obtained at fixed discharge voltage and beam current conditions. These data were taken to identify the optimum discharge operating condition for a given beam current. This optimum condition was defined to be the 'knee' of the discharge losses versus propellant efficiency curve.

Thruster Test Results

This section discusses performance assessments of both the FM and EM thrusters and includes the results of direct-thrust measurements obtained with the FMT, power-throttling data for the FMT over a 0.5-2.3 kW envelope, and preliminary performance data for the EMT.

Direct Thrust Measurements

Direct thrust measurements were obtained with the FMT over an input power range of 0.29-2.3 kW to verify thrust-loss estimates associated with beam divergence and multiply-charged ions. Figure 3 shows the FMT mounted on the thrust stand. The thrust measurements were obtained in the fashion as previously described and the thrust was also calculated from the measured thruster electrical parameters at each test point in the manner described in the appendix.

A total of 35 separate operating points were examined, including those conditions listed in Table 3, as well as conditions with large excursions in R-ratio (from 0.9 to 0.3) to examine the thrust-loss associated with beam divergence and large variations in discharge chamber propellant efficiency (from 86% to 97%) to examine the thrust-loss associated with doubly-charged ions.

Figure 4 plots the measured thrust values versus the calculated thrust values for all the 35 test points. All values are within the estimated uncertainties of $\pm$ 1.0 mN for the thrust stand measurements and $\pm$ 2.3% for the calculated thrust values. A linear correlation coefficient of 1.0 is obtained for the data. The range of thrust levels varied from approximately 89 mN at 2.3 kW, down to about 12 mN at 0.29 kW. Total thrust-loss correction factors of 0.974 to 0.952 for variations in R-ratio and from 0.971 to 0.953 for variations in discharge propellant efficiency were determined from the thrust measurements. Figure 4 indicates that the calculations of thrust value and the associated correction factors can be used to accurately estimate thruster performance under both nominal and off-normal operating conditions.

FMT Performance

Prior assessments of the FMT were conducted to verify the operation of the aluminum, partial-conic discharge chamber design, evaluate stability, and quantify overall thruster performance in the 0.7-4.9 kW power envelope. These results are reported in Reference 15. In this investigation, performance data for the FMT were obtained over a 0.5-2.3 kW power envelope using an alternative throttling scheme. These tests were conducted to evaluate the efficacy of power-throttling with fixed propellant flow rates to both the discharge and neutralizer cathodes, while varying the main plenum flow rate, discharge current, and ion optics voltages as required.

Thruster performance data at six discrete operating points using this fixed cathode flow rate throttling approach are shown in Figure 5, a plot of thruster efficiency versus specific impulse. Also shown on this figure is the performance envelope for the FMT over a 0.7-4.9 kW power range obtained using variable flow rates through the cathodes (from Ref. 15). The vertical range in the envelope is associated with the fact that the performance curve is sensitive to beam current, since the discharge losses are sensitive to beam current. For power levels greater than approximately 1.0 kW, the fixed flow throttling approach achieves efficiencies comparable to that obtained by varying the cathode flow rates at each condition. For power levels below about 1.0 kW, the thruster efficiency drops off markedly due to the rather large magnitude of the neutralizer propellant flow rate and input power.

The thruster operating parameters for the six data points identified in Figure 5 are listed in Table 3. Of interest to note is that efficient power-throttling was demonstrated over a 4.3:1 power range using this fixed flow rate approach, with efficiencies varying from 66% at 2.32 kW input power, down to 36% at 0.54 kW. Additionally, this range was accomplished with only 2 accelerator grid voltage set points and at a maximum magnitude of 180 volts.

Additional performance tests were conducted with the FMT to evaluate it's maximum efficiency at power levels in the range of approximately 0.5-1.0 kW. Figure 6 shows the FMT efficiency versus input power for the six data points at fixed cathode flow rates. Additionally, maximum efficiency conditions at six power levels between 0.5-1.0 kW are also plotted, where the propellant

flow rates and ion optics voltages were established discretely at each condition. These data range from a minimum efficiency of 49% at 530 W to a maximum efficiency of 64% at 950 W. While these data are at substantially higher efficiency than those obtained at fixed cathode flow rate conditions (approximately 13 percentage points higher at 0.53 kW and 14 percentage points higher at 1.0 kW), they were obtained at higher specific impulse and hence lower thrust. For example, at 1.0 kW input power, the high efficiency thruster condition yields 31 mN thrust at 4160 seconds specific impulse, while the lower efficiency fixed-cathode flow rate condition yields 44 mN thrust at 2530 second. It is anticipated that improvements in thruster efficiency in the power range of 0.5-1.0 kW could be attained via redesign of the neutralizer. An increase in approximately 5 percentage points (to 53%) at 0.5 kW and approximately 3 percentage points (to 67%) at 1.0 kW could be realized by reduction in the neutralizer steady-state input power.

EMT Performance

To date, preliminary performance assessments of the EMT have been conducted at input power levels of approximately 2.30 kW, 1.45 kW, and 0.58 kW to evaluate discharge chamber, neutralizer, ion optics, and overall thruster operation. These power levels were obtained using the same throttling scheme employed with the FMT; namely, by fixing the cathode propellant flow rates and varying the main plenum flow rate, cathode emission current, and ion optics voltages as necessary. Figure 7 plots the efficiency versus specific impulse obtained with the EMT, along with that for the FMT. As noted, the performance of the EMT compares favorably to the earlier-generation thruster.

Table 4 lists in detail the performance and operating parameters for the FMT and EMT for operation at 2.3 kW. Typical performance for the EMT is a 65% efficiency, a thrust of 93 mN, and a specific impulse of 3280 seconds. Some improvement in the discharge chamber electrical efficiency of the EMT is noted over that of the FMT (155 W/A versus 188 W/A) and this is believed due to modifications made to the magnetic circuit. Preliminary data indicate no substantial difference in perveance or electron backstreaming limit between the two ion optics designs.

Thruster Lifetime Expectations

For the NASA 30 cm thruster, the erosion of the molybdenum accelerator grid due to charge-exchange processes is the dominant life limiting wear-mechanism. The accelerator grid is the minimum-life component for most of the thruster operational envelope, and thus the thruster operating levels are derated to insure long life. Under most ground test conditions for high power ion thrusters, a significant fraction of the accelerator impingement current is due to charge-exchange ions from residual propellant atoms in the facility. The charge-exchange erosion patterns have been described in detail[19,20] and several recent models of accelerator grid charge exchange ion erosion have been developed to explain the phenomena.[21-23] Examinations of accelerator grid erosion on many different ion thrusters have led to a consensus that the ultimate end-of-life of an accelerator grid will be determined by structural failure in the center of the grid where the erosion is the greatest. In particular, erosion occurs nonuniformly around each grid hole to form deep pits which are connected together by shallower trenches.[19] Erosion in the trenches is minimum between two adjacent charge-exchange pits. After significant erosion occurs, each grid hole is bridged to its six neighbors at these minimum erosion sites.[20] Ultimate end-of-life of the accelerator grid is thereby defined as the point in time at which these bridges in the center of the grid become unsound and fail. However, in over 30 years of testing, no accelerator grid has ever suffered sufficient charge-exchange erosion to fail in this manner.

The relevant local measurement for this accelerator grid end-of-life mechanism is the bridge depth erosion in the center of the accelerator grid. A compilation of the magnitude of accelerator grid erosion experienced during extended-duration tests,[4,5,24-26] along with the thruster operating conditions, are listed in Table 5. Where accelerator grids were available for direct inspection, an average erosion depth was obtained from the six bridge erosion measurements made around the center hole. A "grid erosion parameter" which consisted of the product of the accelerator grid impingement current, test time, and grid material sputter yield, divided by the beam area was selected as the most straightforward combination of measured parameters with the highest correlation to the magnitude of the charge exchange erosion. Table 5 includes data only for extended tests where there were sufficient pre- and post-test documentation to provide a high fidelity estimate of both the erosion and the grid erosion parameter.

Figure 8 plots the average bridge erosion depth about the accelerator grid center hole as a function of the grid erosion parameter for the several extended-duration tests listed in Table 5. While charge exchange ion erosion involves many details not explicitly included in this simple parameter, (such as the effects of variations in charge exchange ion density profiles, grid geometry, erosion patterns, facility backsputtered material, net sputtering rate due to changes in the ion angle of incidence, redeposition of sputtered grid material, and so on), the grid erosion parameter appears to account for the details of the erosion processes and quite accurately describes the critical phenomemon. For example, the erosion data used in Figure 8 were taken in ground tests over conditions where the facility effects ranged from quite noticeable to nearly negligible. There is no ques-

tion that high background test pressures increase the total accelerator grid erosion rates, but the critical erosion phenomena appears to be well described by the grid erosion parameter which simply and adequately accounts for the facility effects by including the observed accelerator grid impingement current.

Although the data from Figure 8 provide measured erosion, it is necessary to define a credible safety factor for the EM thruster and the accelerator grid from Reference 5 provides a conservative basis for that estimate. This accelerator grid accumulated 1560 hours on a 30 cm diameter ion thruster with an accelerator grid thickness nearly identical to that of the EM thruster. It experienced erosion of about 230 microns, about 40 percent through the grid, but is still very robust and is in excellent operating condition with many more hours of operating time left. Based on this experience, an erosion depth of 200 microns (40 percent of the EMT accelerator grid thickness) is selected as the end-of-useful life condition. The conservativeness of this selection is supported by the results from Reference 20 where the accelerator grid was still functioning even though the bridge erosion depth in the center of the grid was typically 70 percent of the 360 micron thick grid.

Figure 8 allows a conservative estimate of accelerator grid end-of-life at operating conditions of interest. The grid erosion parameter for the EM thruster operating in space for 10 khr at 2.3 kW is about 20 ma-h/cm^2. Ten thousand hours is at least 1.6 times that required for a 15 year north-south stationkeeping and repositioning mission of a 5000 kg class spacecraft.[27] From Fig. 8 the expected erosion depth is only 100 microns or half the end-of-useful life value, after this operating time. Extended-duration tests of the EM thruster are required to provide decision makers the degree of statistical credibility of overall thruster reliability in its proposed manifestation.

EMT Thruster Weartest and Component Life Testing

A 2000 hour test of the EMT on xenon propellant will be initiated shortly at NASA LeRC at a nominal 2.3 kW input power. This test will be conducted to obtain long term performance and wear data in a ground test facility that simulates the relevant space environment and to insure the transportability of life test data from one facility to another. The objectives of the test are to: demonstrate 2000 hours of continuous service life at a thruster input power of 2.3 kW and identify life-limiting phenomena; obtain wear, erosion, and surface deposition data relevant to potential thruster/spacecraft interactions; validate the adequacy of process documents for the thruster, vacuum facility, propellant feed system, power processor, and test procedures; and provide input to flight thruster design requirements.

A test program is on-going to develop and validate hollow cathode technology for the space station plasma contactor program.[28] Much of the technology and cathode components for the thruster are common with the plasma contactor including the cathode insert, the neutralizer, and heater subassemblies. Hence, much of the life test and performance data derived from the hollow cathode contactor activity is directly transportable to the engineering model thruster development. These activities include hollow cathode and heater life testing and validation, definition and validation of contamination control protocols and procedures implemented in the propellant management system, definition and verification of conditions for cathode ignition, and development of cathode storage, handling, and activation requirements.

Concluding Remarks

A 30 cm diameter xenon ion thruster is under development at NASA to provide an ion propulsion option for auxiliary and primary propulsion on missions of national interest. Under this program the ion thruster has been brought to engineering model development status. Goals of this development effort included a thruster mass of 7 kg and an operating power envelope of 0.5 to 2.3 kW. The overall mass of the EMT, including 3 m cable harness, is approximately 6.4 kg and is somewhat lighter than it's predecessor. The thruster incorporates major innovations in structural design, materials, and fabrication techniques compared to those employed in conventional ion thrusters.

Performance assessments of both a functional model and the engineering model thruster were conducted, and these included direct-thrust measurements obtained with the FMT, power-throttling data for the FMT over a 0.5-2.3 kW envelope, and preliminary performance data for the EMT. Direct thrust measurements were obtained with the FMT over an input power range of 0.29-2.3 kW to verify thrust-loss estimates associated with beam divergence and multiply-charged ions. A total of 35 separate operating conditions were examined, including conditions with large excursions in R-ratio (from 0.9 to 0.3) to examine the thrust-loss associated with off-axis vectoring and large variations in discharge chamber propellant efficiency (from 86% to 97%) to examine the thrust-loss associated with doubly-charged ions. The calculations of thrust, based on measured electrical parameters of the thruster, were in excellent agreement with the thrust stand measurements. These results indicate that the calculations of thrust value and the associated correction factors can be used to accurately estimate thruster performance under both nominal and off-nominal operating conditions.

Performance data for the FMT were obtained over a 0.5-2.3 kW power envelope using an alternative throttling scheme. These tests were conducted to evaluate the efficacy of power-throttling with fixed propellant flow rates to both the discharge and neutralizer cathodes, while varying the main plenum flow rate, discharge current, and

ion optics voltages as required. Efficient power-throttling was demonstrated over a 4.3:1 power range using this fixed flow rate approach, with efficiencies varying from 66% at 2.32 kW input power, down to 36% at 0.54 kW. Additionally, this range was accomplished with only two accelerator grid voltage set points and at a maximum magnitude of 180 volts. Additional performance tests were conducted with the FMT to evaluate it's maximum efficiency at power levels in the range of approximately 0.5-1.0 kW, and peak efficiencies of 49% at 530 W and 64% at 950 W were demonstrated.

Preliminary performance assessments of the EMT were conducted at input power levels of approximately 2.30 kW, 1.45 kW, and 0.58 kW to evaluate discharge chamber, neutralizer, ion optics, and overall thruster operation and these data compare favorably to the earlier-generation FM thruster. Typical performance for the EMT is a 66% efficiency, a thrust of 93 mN, and a specific impulse of 3280 seconds, at 2.3 kW input power.

For the NASA 30 cm thruster, the erosion of the molybdenum accelerator grid due to charge-exchange processes is the dominant life limiting wear-mechanism. The relevant local measurement for this accelerator grid end-of-life mechanism is the bridge depth erosion in the center of the accelerator grid. An examination of the accelerator grid erosion data from several extended-duration tests indicate that a simple grid erosion parameter which consisted of the product of the accelerator grid impingement current, test time, and grid material sputter yield, divided by the beam area provides a high correlation to the magnitude of the measured charge exchange erosion. While charge exchange ion erosion involves many details not explicitly included in this simple parameter, it appears to account for the details of the erosion processes and quite accurately describes the critical phenomemon. Based on this parameter, the end of useful life of the EMT at 2.3 kW is estimated to be 20,000 h.

Extended-duration tests of the EM thruster are, of course, required to provide decision makers the degree of statistical credibility of overall thruster reliability in its proposed manifestation. As such, a 2000 hour test of the EMT on xenon propellant will be initiated shortly at NASA Lewis at a nominal 2.3 kW input power. This test will be conducted to demonstrate 2000 hours of continuous service life at a thruster input power of 2.3 kW, and identify life limiting phenomena and to provide input to flight thruster design requirements.

Acknowledgements

The authors would like to express their appreciation to Eli Green, George Jacynycz, Craig Nelson, and Eugene Pleban for test support, thruster assembly and suggestions in design.

References

[1]Groh, K., "Development Status of the RIT Ion Engines, " AIAA Paper No. 90-2671, July 1990.

[2]Fearn, D.G., "The Proposed Demonstration of the UK-10 Ion Propulsion System on ESA's SAT-2 Spacecraft," IEPC Paper No. 88-031, October 1988.

[3]Kajiwara, K. and Katada, M., "Test Facilities for the ETS-VI Ion Engine System," AIAA Paper No. 90-2656, July 1990.

[4]Patterson, M.J. and Verhey, T.R., "5kW Xenon Ion Thruster Lifetest," AIAA Paper No., 90-2543, July 1990.

[5]Rawlin, V.K., "Internal Erosion Rates of a 10-kW Xenon Ion Thruster," AIAA Paper No. 88-2192, July 1988.

[6]Patterson, M.J. and Rawlin, V.K., "Performance of 10-kW Class Xenon Ion Thrusters," AIAA Paper No. 88-2914, July 1988.

[7]Patterson, M.J. and Williams, G.J. Jr., "Krypton Ion Thruster Performance," AIAA Paper No. 92-3144, July 1992.

[8]Sovey, J.S., "Improved Ion Containment Using a Ring-Cusp Ion Thruster," *Journal of Spacecraft and Rockets*, Vol. 21, Sept.-Oct. 1984, pp. 488-495.

[9]Patterson, M.J. and Rawlin, V.K., "Derated Ion Thruster Design Issues," IEPC Paper No. 91-150, October 1991.

[10]Rawlin, V.K., "Characterization of Ion Accelerating Systems on NASA's Ion Thrusters," AIAA Paper No. 92-3827, July 1992.

[11]Patterson, M.J. and Mohajeri, K., "Neutralizer Optimization," IEPC Paper No. 91-151, October 1991.

[12]Patterson, M.J., "Low-Isp Derated Ion Thruster Operation," AIAA Paper No. 92-3203, July 1992.

[13]Verhey, T.R. and Patterson, M.J., "Microanalysis of Extended-Test Xenon Hollow Cathodes," AIAA Paper No. 91-2123, June 1991.

[14]Sarver-Verhey, T.R., "Extended Testing of Xenon Ion Thruster Hollow Cathodes," AIAA Paper No. 92-3204, July 1992.

[15]Patterson, M.J., Haag, T.W., and Hovan, S.A., "Performance of the NASA 30 cm Ion Thruster," IEPC Paper No. 93-108, September 1993. (Also NASA TM-1064226).

[16]30-Centimeter Ion Thruster Subsystem Design Manual," NASA TM-79191, June 1979.

[17]Rawlin, V.K. and Majcher, G., "Mass Comparisons of Electric Propulsion Systems for NSSK of Geosynchronous Spacecraft," AIAA Paper No. 91-2347, June 1991.

[18]Rawlin, V.K., Pinero, L., and Hamley, J., "Simplified Power Processing for Inert Gas Ion Thrusters," AIAA Paper No. 93-2397, June 1993.

[19]Rawlin, V.K., "Erosion Characteristics of Two-Grid Ion Accelerating Systems," IEPC Paper No. 93-175, September 1993.

[20]Brophy, J.R., Polk, J.E., and Pless, L.C., "Test-to-

Failure of a Two-Grid, 30 cm dia. Ion Accelerator System," IEPC Paper No. 93-172, September 1993.

[21]Monheiser, J.M. and Wilbur, P.J., "Effects of Design and Operating Conditions on Accelerator-Grid Impingement Current," IEPC Paper No. 93-174, September 1993.

[22]Polk, J.E., Moore, N.R., Newlin, L.E., Brophy, J.R., and Ebbeler, D.H., "Probabilistic Ion Engine Service Life Assessment," IEPC Paper No. 93-176, September 1993.

[23]Peng, X., Ruyten, E., and Keefer, D., "Parametric Study of Grid Erosion Patterns in Two-Grid Ion Thrusters," IEPC Paper No. 93-173, September 1993.

[24]Dulgeroff, C.R., Beattie, J.R., Poeschel, R.L., and Hyman, J., "Ion Thruster System (8-CM) Cyclic Endurance Test," NAS3-21741, October 1984.

[25]Kitamura, S., Miyazaki, K., and Hayakawa, Y., "1000 Hour Test of 14 cm Diameter Ring-Cusp Xenon Ion Thruster," AIAA Paper No. 90-2542, July 1990.

[26]Collett, C., "Thruster Endurance Test," NAS3-15523, May 1976.

[27]Oleson,S.R., personal communication, NASA Lewis Research Center, June 1994.

[28]Patterson, M.J., Hamley, J., Sarver-Verhey, T., and Soulas, G., "Functional Testing of the Space Station Plasma Contactor," AIAA Paper No. 94-3308, June 1994.

Appendix A

Performance Calculations -

The following equations and assumptions were used in the calculation of thrust:

- Thrust, in mN -

$$F = \gamma \left(2\frac{m}{q}\right)^{1/2} J_b \left(V_b\right)^{1/2}. \qquad (1)$$

The total thrust-loss correction factor is given by

$$\gamma = \alpha F_t. \qquad (2)$$

The correction factor for doubly-charged ions is calculated from the equation

$$\alpha = \frac{\left(1 + 0.7071 \frac{I^{++}}{I^{+}}\right)}{\left(1 + \frac{I^{++}}{I^{+}}\right)}. \qquad (3)$$

As a spectrometer probe was not available during this investigation, beam-centerline current data for a similar type thruster operating on xenon, correlated to discharge chamber propellant utilization efficiency, was used for this analyses.[A1] The use of this centerline data is expected to yield a worst-case correction factor. The thrust-loss correction factor for off-axis vectoring was calculated from the polynomial equation

$$F_t = \Delta Ft - 0.1470 + 0.8440(R) - 2.0675(R)^2 + 2.3661(R)^3 - 1.0167(R)^4, \qquad (4)$$

obtained from a curve fit of experimental data of Danilowicz, et. al..[A2] In equation 4, R is the ratio of net-to-total accelerating voltage. An additional term ΔF_t is included as a normalization constant to take into account thrust-loss dependency on ion optics electrode geometry. This term is a product of three correction factors, one each for the accelerator-to-screen grid aperture diameter ratio, accelerator grid thickness-to-screen grid diameter ratio, and the grid gap-to-screen grid aperture diameter ratio. The values of these correction factors were obtained from curves fits of experimental data of Kaufman.[A3]

The beam voltage in equation 1 is given by

$$V_b = V_s + - \left| V_g \right|. \qquad (5)$$

Note that the output of the screen power supply is tied to the positive side of the discharge power supply in the present test configuration.

In general the overall uncertainty in the thrust may be expressed as

$$\frac{\Delta F}{F} = \left[\left(\frac{\Delta \gamma}{\gamma}\right)^2 + \left(\frac{\Delta J_b}{J_b}\right)^2 + \frac{1}{4}\left(\frac{\Delta V_b}{V_b}\right)^2\right]^{1/2},$$

where the terms on the right hand side of the equation represent the uncertainties in the total thrust-loss correction factor, the beam current, and the beam voltage. These uncertainties are estimated to be 2%, 1%, and 1%, respectively, resulting in an overall uncertainty in the thrust of ±2.3%.

References

[A1]Rawlin, V.K., "Operation of the J-Series Thruster Using Inert Gas," NASA TM-82977, November 1982.

[A2]Danilowicz, R.L., et. al., "Measurement of Beam Divergence of 30-Centimeter Dished Grids," AIAA Paper No. 73-1051, October 1973.

[A3]Kaufman, H.R., "Accelerator-System Solutions for Electron Bombardment Ion Sources," March 1975.

Table 1 FMT and EMT Design Attributes

Attribute	FM Thruster	EM Thruster
Mass, kg	6.9	6.4
Structural Material	Al 1100	Al 5052 and Ti AMS 4901
Assembly Fasteners	machine screws	blind rivots
Propellant Isolators	low pressure-high voltage	high pressure-high voltage

Table 2 FMT and EMT Ion Optics Electrode Designs

electrode design	electrodes	
attribute	screen	accelerator
electrode thickness, mm	0.38	0.38 (FMT) 0.51 (EMT)
hole diameter, mm	1.91	1.14
open-area-fraction	0.67	0.24

Table 3 - FMT Power-Throttling Performance at Fixed Cathode Propellant Flow Rates

Input Power, kW	Beam Current, A	Specific Impulse, s	Thrust, mN	Efficiency,	Mass Flow Rate, mg/s	Screen Voltage, V	Accel Voltage V
2.32	1.72	3380	91	0.66	2.75	1110	180
1.75	1.54	2650	75	0.56	2.90	910	180
1.51	0.95	3170	55	0.57	1.80	1310	150
1.09	0.91	2530	44	0.50	1.80	910	150
0.95	0.58	2660	34	0.47	1.30	1310	150
0.54	0.54	1760	22	0.36	1.30	650	150

Table 4 - Comparison of Typical FM and EM Thruster Performance at 2.3 kW

Parameter	FM Thruster	EM Thruster
Input power, W	2320	2290
Thrust, mN	91	93
Specific Impulse, s	3380	3280
Overall Thruster Efficiency, %	66	65
Xenon Mass Flow Rate, mg/s	2.75	2.89
Total Propellant Efficiency, %[1]	83	81
Beam Current, A	1.72	1.77
Screen Voltage, V	1110	1110
Accel Grid Impingement Current, mA	7.7	8.8
Accel Voltage, V	-180	-180
Discharge Voltage, V	26	26
Cathode Emission Current, A	12.5	10.9
Discharge Losses, W/A	188	161
Discharge Propellant Efficiency, %[1]	92	92
Neutralizer Keeper Voltage, V	16.0	17.3
Neutralizer Keeper Current, A	2.0	2.0
Coupling Voltage, V[2]	-17	-14

[1]Total and discharge propellant efficiencies corrected for propellant ingested from facility, and for doubly-charged ions.
[2]Coupling voltage approximated by measurement of the floating potential of neutralizer cathode-common with respect to facility ground.

Table 5 - Accelerator Grid Erosion Data

Ref.	Thruster Dia., cm	Thruster Input Power, kW	Propellant	Beam Area, cm^2	Accel Grid Thickness, microns	Accel Voltage, V	Accel Grid Impingement Current, mA	Total Test Time, h
24	8	0.13	Hg	52	510	-290 -290	0.27 0.49	2100 7400
25	14	0.62	Xe	154	500	-800	1.73	983
19	30	2.7 3.0	Hg Xe	642	510	-300 -300	3.7 10	6210 200
26	30	2.0	Hg	642	500	-500	2.8	10,000
19	30	2.7 3.0	Hg Xe	642	380	-300 -300	4 10	1433 100
5, 19	30	2.7 10 5-10	Hg Xe Xe	642	570	-300 -510 -500	4 47 25	520 740 300
4	30	5.5	Xe	642	360	-330	17.4	1160

Table 5 continued - Accelerator Grid Erosion Data

Ref.	Sputter Yield, atoms/ion	Grid Erosion Param., $mA\text{-}h/cm^2$	Background Pressure, Pa x 10^{-4}	Avg. Bridge Erosion Depth, microns
24	0.26 0.26	20.9	0.4	110
25	1.0	11.0	3	43
19	0.26 0.50	10.9	4.7 10	50
26	0.70	30.5	2	150
19	0.26 0.50	3.1	4.7 10	0
5, 19	0.26 0.88 0.88	43[1]	4.7 10 10-20	230
4	0.51	16	17	80

[1]Corrected for downstream surface erosion beyond trenches.

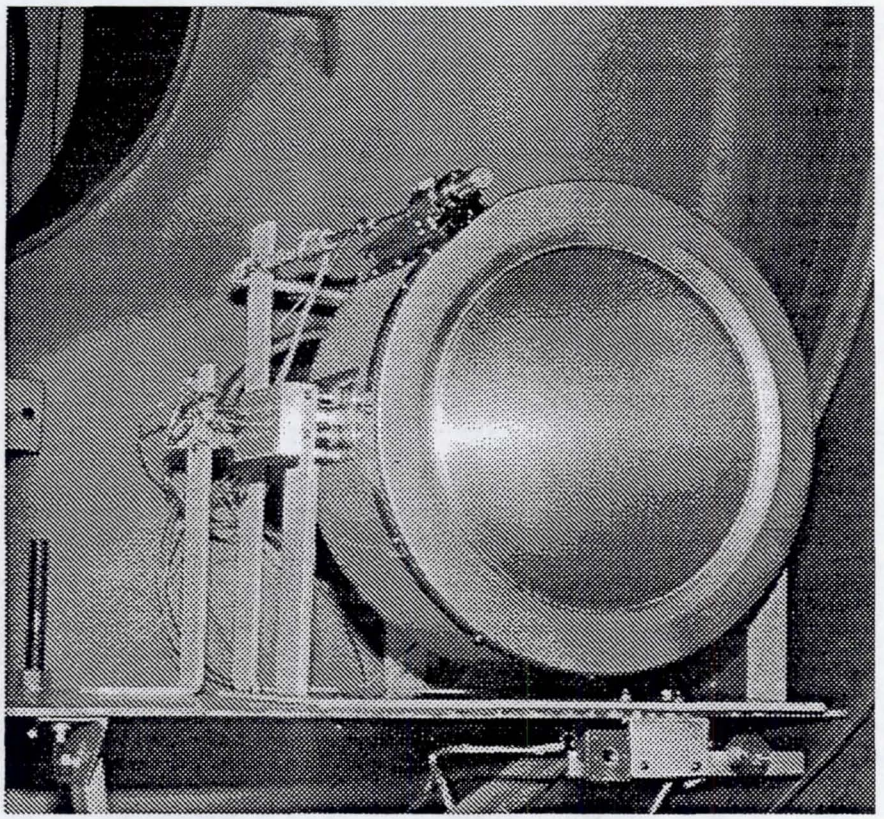

Fig. 1 Engineering model thruster; front view.

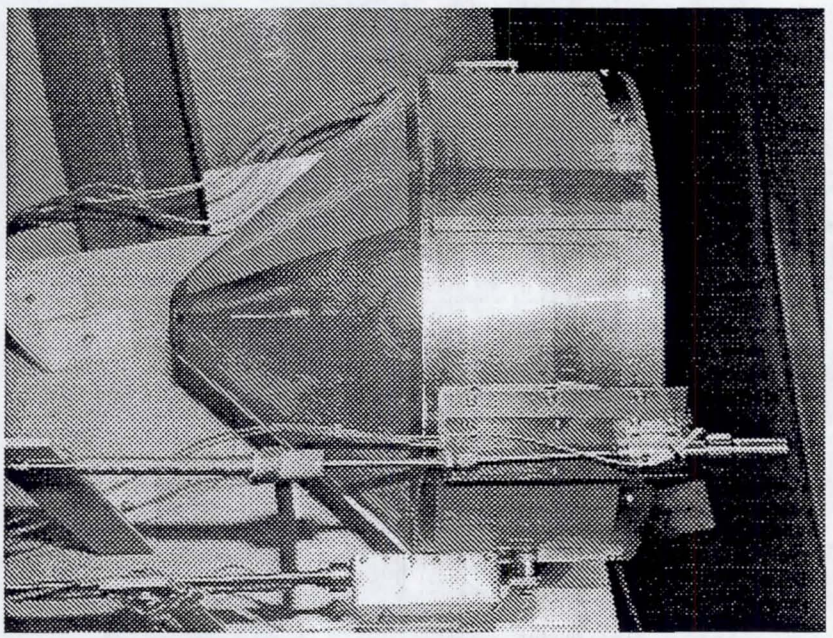

Fig. 2 Engineering model thruster; side view.

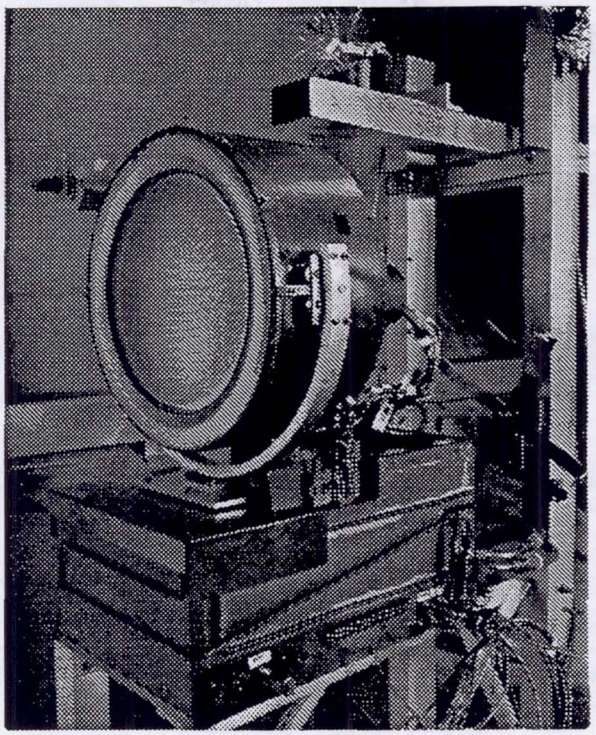

Fig. 3 Functional model thruster mounted on thrust-stand.

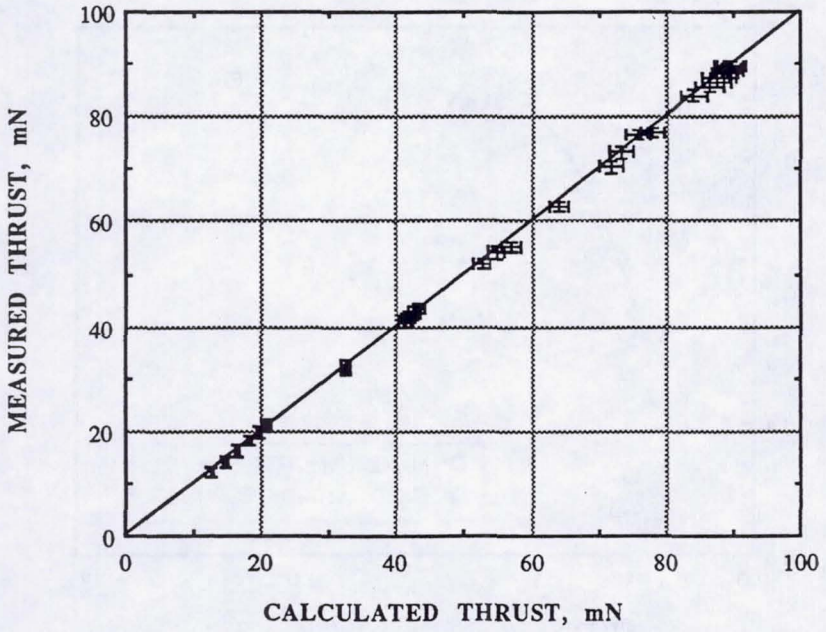

Fig. 4 Measured versus calculated thrust levels for FM thruster.

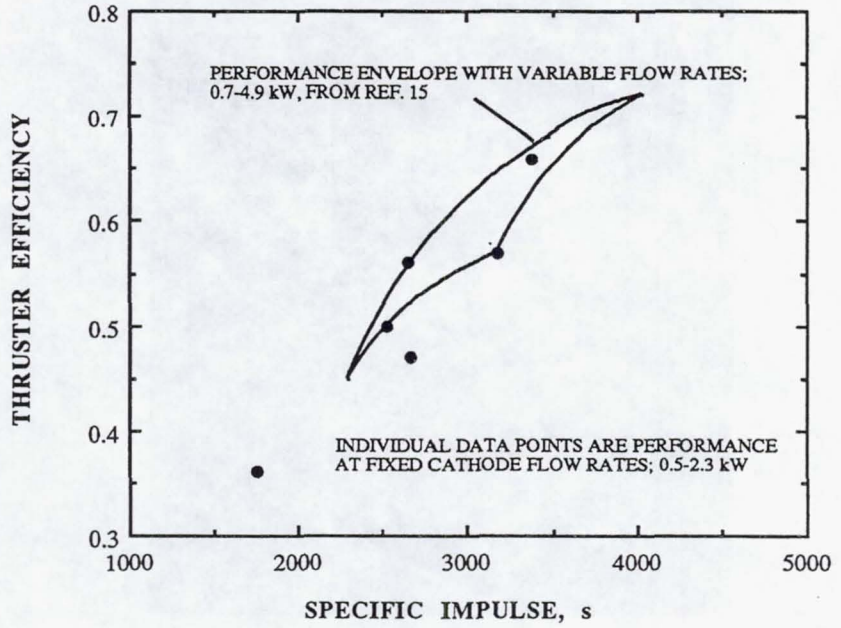

Fig. 5 Comparison of FM thruster performance with variable and fixed cathode flow rates.

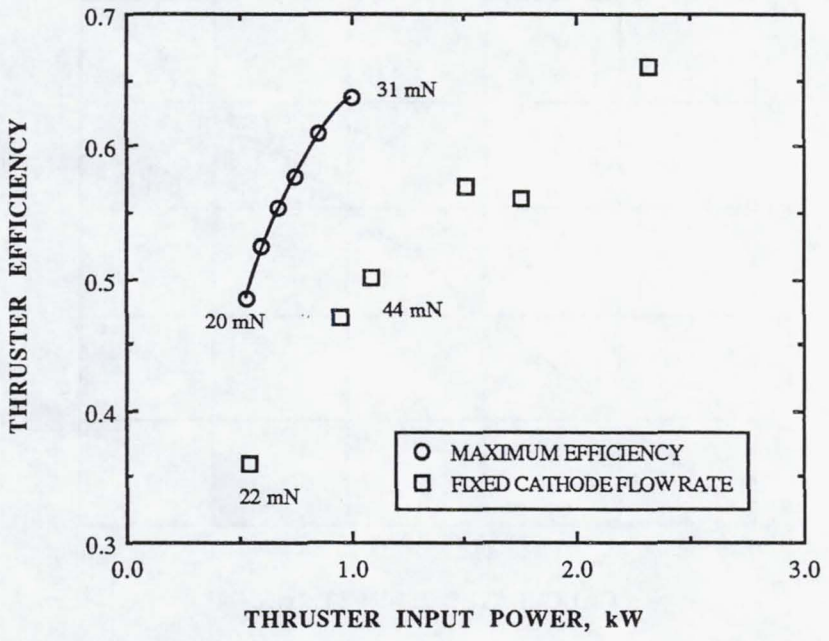

Fig. 6 FMT maximum efficiency at 0.5-1.0 kW; thrust levels noted.

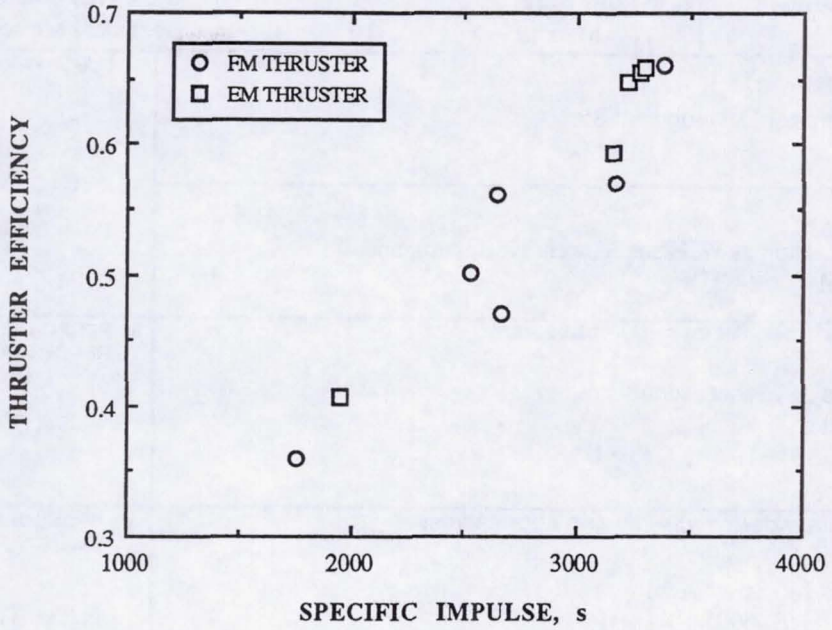

Fig. 7 Comparison of EMT and FMT performance.

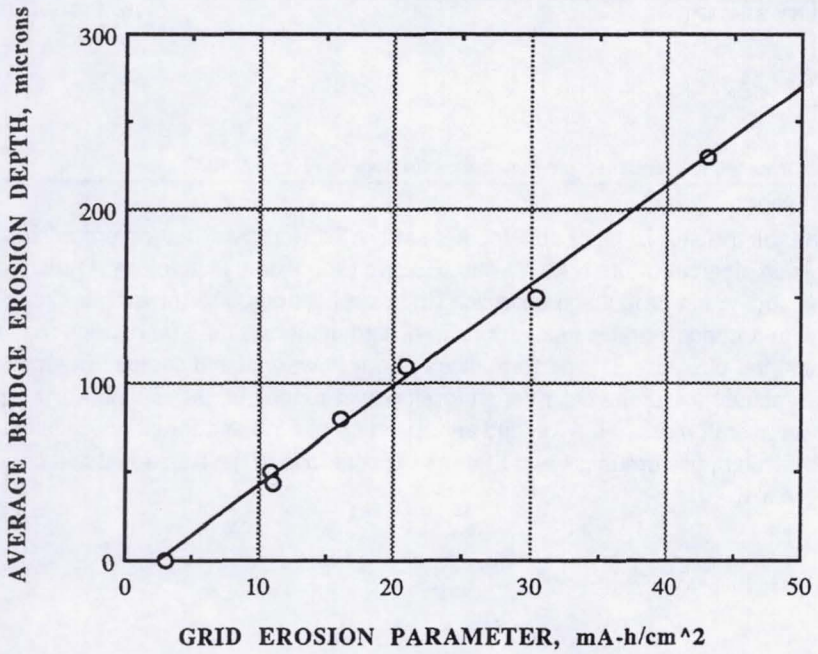

Fig. 8 Correlation of grid center erosion depth with grid erosion parameter.

REPORT DOCUMENTATION PAGE

Form Approved
OMB No. 0704-0188

1. AGENCY USE ONLY (*Leave blank*)	2. REPORT DATE	3. REPORT TYPE AND DATES COVERED
	March 1995	Technical Memorandum

4. TITLE AND SUBTITLE

NASA 30 cm Ion Thruster Development Status

5. FUNDING NUMBERS

WU-232-02-03

6. AUTHOR(S)

Michael J. Patterson, Thomas W. Haag, Vincent K. Rawlin, and
Michael T. Kussmaul

7. PERFORMING ORGANIZATION NAME(S) AND ADDRESS(ES)

National Aeronautics and Space Administration
Lewis Research Center
Cleveland, Ohio 44135-3191

8. PERFORMING ORGANIZATION REPORT NUMBER

E-9406

9. SPONSORING/MONITORING AGENCY NAME(S) AND ADDRESS(ES)

National Aeronautics and Space Administration
Washington, D.C. 20546-0001

10. SPONSORING/MONITORING AGENCY REPORT NUMBER

NASA TM-106842
AIAA-94-2849

11. SUPPLEMENTARY NOTES

Prepared for the 30th Joint Propulsion Conference cosponsored by AIAA, ASME, SAE, and ASEE, Indianapolis, Indiana, June 27-29, 1994. Michael J. Patterson, Thomas W. Haag, and Vincent K. Rawlin, NASA Lewis Research Center; Michael T. Kussmaul, NYMA, Inc., Engineering Services Division, 2001 Aerospace Parkway, Brook Park, Ohio 44142 (work funded by NASA Contract NAS3-27186). Responsible person, Michael J. Patterson, organization code 5330, (216) 433-7481.

12a. DISTRIBUTION/AVAILABILITY STATEMENT

Unclassified - Unlimited
Subject Category 20

This publication is available from the NASA Center for Aerospace Information, (301) 621-0390.

12b. DISTRIBUTION CODE

13. ABSTRACT (*Maximum 200 words*)

A 30 cm diameter xenon ion thruster is under development at NASA to provide an ion propulsion option for missions of national interest and it is an element of the NASA Solar Electric Propulsion Technology Applications Readiness (NSTAR) program established to validate ion propulsion for space flight applications. The thruster has been developed to an engineering model level and it incorporates innovations in design, materials, and fabrication techniques compared to those employed to conventional ion thrusters. The performance of both functional and engineering model thrusters has been assessed including thrust stand measurements, over an input power range of 0.5-2.3 kW. Attributes of the engineering model thruster include an overall mass of 6.4 kg, and an efficiency of 65% and thrust of 93 mN at 2.3 kW input power. This paper discusses the design, performance, and lifetime expectations of the functional and engineering model thrusters under development at NASA.

14. SUBJECT TERMS	15. NUMBER OF PAGES
Ion thruster	17
	16. PRICE CODE: A03

17. SECURITY CLASSIFICATION OF REPORT	18. SECURITY CLASSIFICATION OF THIS PAGE	19. SECURITY CLASSIFICATION OF ABSTRACT	20. LIMITATION OF ABSTRACT
Unclassified	Unclassified	Unclassified	